Analytic Modeling of Impermeable and Resistant Barriers

by Charles R. Fitts[a]

Abstract

Superpositioned analytic functions are used to efficiently and accurately model ground-water flow fields containing thin barriers such as slurry walls and sheet-pile walls. Barriers are modeled as a series of straight-line segments strung together to create irregularly shaped open or closed boundaries with zero thickness. The complex analytic functions employed provide perfect continuity of flow across the boundary while approximating normal flux boundary conditions along the boundary. Along an impermeable boundary the normal flux is specified as zero, and along a resistant (leaky) barrier the normal flux is proportional to a specified resistance parameter and the potential difference across the boundary. Solution of a given flow problem requires solving a system of equations with one equation per boundary corner. These equations are linear for impermeable boundaries and for resistant boundaries in confined aquifers or single-strata unconfined aquifers. In other cases, the boundary condition equations associated with resistant barriers can be nonlinear and a new technique for iterative solution is employed. Implementation of these techniques in a computer program is tested and it is demonstrated by modeling various configurations of flow funneled into a gap between two barriers.

Introduction

Barriers to flow such as slurry walls and sheet-pile walls are often important features in the ground-water flow fields at contaminated sites and at construction sites. These barriers are typically vertical and very thin compared to their horizontal extent. The hydraulic conductivity of the barriers is generally low enough that most flow is deflected around the barrier. In some cases, a significant amount of flow also leaks through the barrier. Barriers have been used to ring contamination sources, and some recent attention has focused on the use of barriers to channel contaminant plumes into a small zone where in situ treatment occurs (Pankow et al., 1993).

Flow around barriers can be modeled with numerical models (e.g. McDonald and Harbaugh, 1988; Hseih and Freckleton, 1993), but to achieve reasonable accuracy requires fine grid or element spacing in the vicinity of the barrier, and extremely fine spacing where flow curls around the end of a barrier. In some modeling studies, the location of the barrier is a design variable; using a numerical model in such cases is tedious because the spatial discretization must be redefined each time the barrier location is changed. With appropriate analytic functions, it is possible to model steady two-dimensional flow around impermeable and resistant (leaky) barriers without the spatial discretization dilemma of numerical models; changing the location of the modeled barrier requires only a quick adjustment of boundary coordinates. Another advantage of analytic methods over numerical methods in this case is relatively fast and accurate computation.

Previous analytic approaches to the problem include those of Strack (1986) and He (1987). Both implemented analytic solutions for modeling thin impermeable and resistant barriers along smooth curves in two-dimensional steady flow fields. Strack (1986) represented barriers as a curve consisting of hyperbola segments, and He (1987) modeled barriers as a curve consisting of line segments and arc segments. The smooth curve approach used by both researchers avoids the difficulty of assigning boundary conditions at corners in the boundary. At corners, the flux normal to the boundary is multivalued, and a normal flux boundary condition cannot be assigned there.

The techniques presented here differ from the previous techniques of Strack (1986) and He (1987) in essentially two aspects. First, the barriers are modeled as a series of connected straight-line segments. A new technique allows boundary conditions to be effectively approximated, despite the multivalued normal flux at corners. Compared to the previous smooth curve techniques, this straight-line method requires simpler input and is simpler to program. A second contribution of this research is extension of the method to cases involving nonlinear boundary conditions on resistant barriers. Nonlinear boundary conditions arise when barriers are in aquifers that are represented as stratified (i.e. two or more strata with different hydraulic conductivity and thickness).

The following sections describe the modeling techniques, their implementation in a computer program, and example applications. The applications include analysis of discharge through "funnel and gate" barrier systems of varying configurations.

[a]Assistant Professor, Geosciences Department, University of Southern Maine, Gorham, Maine 04038.

Received November 1995, revised May 1996, accepted May 1996.

Basic Equations of the Analytic Method

Superposition of large numbers of analytic functions is a technique that has been widely applied to the solution of steady two-dimensional ground-water flow problems [see Strack (1989), Fitts (1985), and Strack and Haitjema (1981a, 1981b)]. Rather than write analytic solutions for head ϕ directly as functions of position, $\phi(x, y)$, analytic solutions for head are written with the aid of a discharge potential Φ: $\phi[\Phi(x, y)]$. This discharge potential is defined in terms of head so that the following equations are always true.

$$Q_x = -\frac{\partial \Phi}{\partial x}, \quad Q_y = -\frac{\partial \Phi}{\partial y} \tag{1}$$

where Q_x and Q_y [L^2/T] are the components of the aquifer discharge vector in the x and y directions, respectively. The aquifer discharge vector (Q_x, Q_y) represents the flow/time passing through a unit-width panel that extends vertically over the entire thickness of the aquifer. Equations (1) are satisfied for a confined aquifer if the discharge potential and head are related as

$$\Phi = kH\phi + C_c \tag{2}$$

where k is the horizontal hydraulic conductivity, H is the aquifer thickness, and C_c is a constant. If the aquifer is unconfined, the discharge potential satisfies (1) with this definition:

$$\Phi = \frac{k}{2}(\phi - b)^2 + C_u \tag{3}$$

where b is the elevation of the aquifer base, and C_u is a constant. Potential-head relationships that satisfy (1) have also been defined for the other aquifer types, including layered confined/unconfined aquifers (Strack, 1989). For the two-strata aquifer pictured in Figure 1, the following potential-head relationships apply:

$$\begin{aligned}
&\Phi = \tfrac{1}{2}k_1(\phi - b_1)^2 && (b_1 \le \phi \le b_2)\\
&\Phi = k_1H_1(\phi - b_1) + \tfrac{1}{2}k_2(\phi - b_2)^2 + C && (b_2 \le \phi \le b_3)\\
&\Phi = k_1H_1(\phi - b_1) + k_2H_2(\phi - b_2) + D && (\phi \ge b_3)
\end{aligned} \tag{4}$$

where C and D are constants

$$\begin{aligned}
C &= -\tfrac{1}{2}k_1H_1^2\\
D &= -\tfrac{1}{2}(k_1H_1^2 + k_2H_2^2)
\end{aligned} \tag{5}$$

With definitions (4) and (5), Φ is continuous as ϕ crosses the aquifer elevation boundaries b_2 and b_3, and equation (1) holds regardless of the head. These potential definitions are used in the models demonstrated later in this paper. Despite the existence of two strata, the model is two-dimensional in the horizontal plane; all resistance is associated with horizontal components of flow and none is associated with vertical components. Since the problem is posed in terms of Φ, not ϕ, the locations where flow transitions between confined flow, unconfined flow in the upper layer, and unconfined flow in the lower layer do not need to be specified as model input but are given as model output.

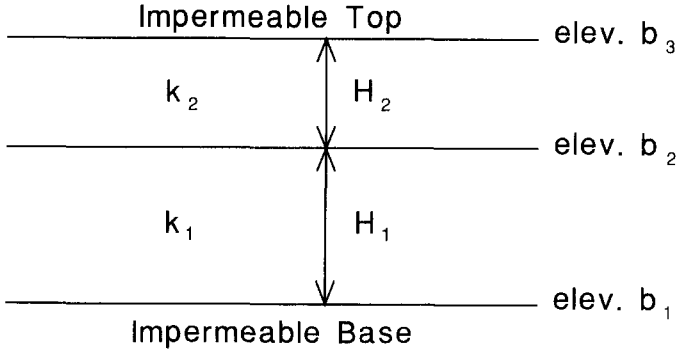

Fig. 1. Two-layered aquifer.

When there is leakage or infiltration into the aquifer from the upper and/or lower boundaries at a net rate N [L/T], continuity of flow requires

$$\frac{\partial Q_x}{\partial x} + \frac{\partial Q_y}{\partial y} = N \tag{6}$$

Combining the continuity condition (6) with (1) gives the Poisson equation, the governing equation for steady flow with infiltration/leakage.

$$\frac{\partial^2 \Phi}{\partial x^2} + \frac{\partial^2 \Phi}{\partial y^2} = \nabla^2 \Phi = -N \tag{7}$$

If there is no leakage/infiltration, the governing equation becomes the Laplace equation.

$$\nabla^2 \Phi = 0 \tag{8}$$

A particular problem is solved by superpositioning discharge potential functions that satisfy the Laplace and/or Poisson equations to yield a composite solution of the governing equation. The total discharge potential Φ_t is a sum of discharge potential functions, each associated with particular boundaries and conditions on those boundaries.

$$\begin{aligned}
\Phi_t(x, y) = {} & g_1\Phi_{g_1}(x, y) + g_2\Phi_{g_2}(x, y) + \ldots\\
& u_1\Phi_{u_1}(x, y) + u_2\Phi_{u_2}(x, y) + \ldots
\end{aligned} \tag{9}$$

Some of the functions contain constant parameters that are given when the problem is posed ($g_1, g_2, \ldots$) and others contain unknown parameters ($u_1, u_2, \ldots$). The coefficient functions $\Phi_{g_1}(x, y)\ldots$ and $\Phi_{u_1}(x, y)\ldots$ are analytic solutions representing the effects of specific aquifer features such as wells or stream segments. The unknown parameters $u_1, u_2, \ldots$ are determined by specifying a number of boundary conditions at control points located on aquifer features or boundaries. The number of specified boundary conditions equals the number of unknown parameters, yielding a system of linear equations which is solved by standard methods.

Analytic expressions for the aquifer discharge vector (Q_x, Q_y) are given by a sum of the derivatives of each potential function.

$$\begin{aligned}
Q_x = -\frac{\partial \Phi_t}{\partial x} = {} & -g_1\frac{\partial \Phi_{g_1}}{\partial x} - g_2\frac{\partial \Phi_{g_2}}{\partial x} - \ldots\\
& -u_1\frac{\partial \Phi_{u_1}}{\partial x} - u_2\frac{\partial \Phi_{u_2}}{\partial x} - \ldots\\
Q_y = -\frac{\partial \Phi_t}{\partial y} = {} & -g_1\frac{\partial \Phi_{g_1}}{\partial y} - g_2\frac{\partial \Phi_{g_2}}{\partial y} - \ldots\\
& -u_1\frac{\partial \Phi_{u_1}}{\partial y} - u_2\frac{\partial \Phi_{u_2}}{\partial y} - \ldots
\end{aligned} \tag{10}$$

These analytic expressions for the aquifer discharge vector are used when specifying boundary conditions on impermeable and

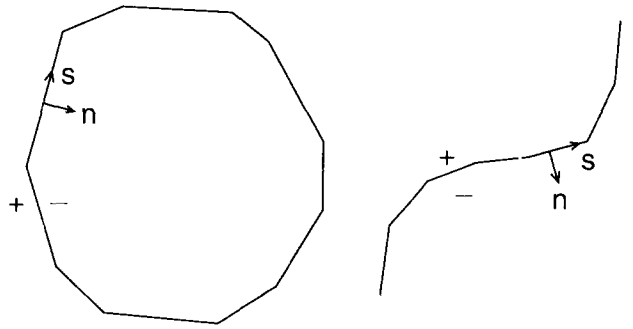

Fig. 2. Open and closed barriers.

resistant boundaries, and when tracing pathlines for model output plots.

Discharge potential functions are available to represent many aquifer features, including infiltration/leakage, uniform crossflow, wells, streams, areal recharge or leakage, thin leaky or draining features and aquifer heterogeneities [see Strack (1989) for detailed descriptions of the method and these functions].

Barrier Modeling Method

Barriers are approximated as a series of straight-line segments that form either open-ended boundaries or closed loop boundaries, as shown in Figure 2. Although actual barriers have small finite width, they are modeled as having no width. Opposite sides of the boundaries are denoted as + and −, n is a local coordinate normal to the boundary, and s is a local coordinate tangential to the boundary.

Potential Functions Representing the Boundary

Each segment of the boundary is represented by a line-doublet complex potential function $\Omega(z) = \Phi + i\Psi$ written as a function of the complex coordinate $z = x + iy$. Line-doublet functions have the following properties suited for modeling of barriers:

- Φ is discontinuous across the boundary ($\Phi^+ \neq \Phi^-$). This is neccessary to produce a discontinuity in head across the boundary.
- The normal component of aquifer discharge is continuous across the boundary ($\partial\Phi^+/\partial n = \partial\Phi^-/\partial n$), which ensures that the boundary itself has no discharge.
- The tangential component of aquifer discharge is discontinuous across the boundary ($\partial\Phi^+/\partial s \neq \partial\Phi^-/\partial s$).

Strack (1989) describes several types of line-doublet functions, two of which are implemented here. All segments other than the tip segments of open-ended boundaries are represented by a function with a linear variation in $(\Phi^+ - \Phi^-)$ along the segment.

$$\Omega = \Phi + i\Psi = \frac{1}{2\pi i}\left[(a_1 Z + a_0)\ln\frac{Z-1}{Z+1} + 2a_1\right] \quad (11)$$

where a_0 and a_1 are real constants, and Z is a dimensionless complex variable defined as

$$Z = \frac{2z - (z_1 + z_2)}{z_2 - z_1} \quad (12)$$

The complex coordinates z_1 and z_2 are at the ends of the line segment, and z is the point where Z and Ω are evaluated. The constants a_0 and a_1 determine the linear distribution of $(\Phi^+ - \Phi^-)$ along the line segment.

The end segments of open-ended boundaries are represented by a line doublet with a square-root distribution of $(\Phi^+ - \Phi^-)$ along its length, which gives the proper boundary conditions around the tip of the element.

$$\Omega = \Phi + i\Psi = \frac{a_0}{2\pi i}\left[(\chi)^{1/2}\ln\frac{(\chi)^{1/2}-1}{(\chi)^{1/2}+1} + 2\right] \quad (13)$$

where a_0 is a real constant, and χ is a dimensionless complex variable defined as

$$\chi = \frac{z - z_1}{z_2 - z_1} \quad (14)$$

The complex coordinate z_1 is at the open end of the line segment, z_2 is at the other end of the line segment, and z is the point where χ and Ω are evaluated.

When the line-doublet functions are strung together to form an irregular boundary, the vartiation in $(\Phi^+ - \Phi^-)$ along the boundary is constrained to be continuous at the junctions between adjacent segments. A hypothetical distribution of $(\Phi^+ - \Phi^-)$ for a four-segment open-ended boundary is illustrated in Figure 3. In this case, there are three unknowns to be solved for: $(\Phi^+ - \Phi^-)$ at each of the three internal corners. Given $(\Phi^+ - \Phi^-)$ at each corner, the constants a_0 and a_1 in the potential functions (11) and (13) can be determined. Whether the boundary is open or closed, the number of unknowns is equal to the number of corners in the boundary. For each of these unknowns, an equation is generated by specifying a normal flux boundary condition associated with each corner.

Figure 4 illustrates what could be considered a unit function associated with a typical corner. Both line segments shown are represented by function (11), with $(\Phi^+ - \Phi^-)$ varying linearly from zero at the ends to 1.0 at the common corner. The composite potential for a series of line segments can be thought of as a series of these unit functions scaled and superpositioned to provide the proper distribution of $\Phi^+ - \Phi^-$ along the boundary. Also shown in Figure 4 is what this unit function contributes to the component of aquifer discharge normal to the right-hand segment, $Q_n = -\partial\Phi/\partial n$. Q_n is continuous across the right-hand segment, as desired. It can also be seen that Q_n is singular at the ends of the segment; the normal flux boundary condition associated with the corner cannot be assigned at the corner. Instead, the normal flux boundary condition is assigned at two control points that straddle the corner, ¼ of the segment length from the corner. The ¼ distance was chosen because the normal flux contributed by the unit function for this corner is large compared to the normal flux contributed by unit functions associated with adjacent corners.

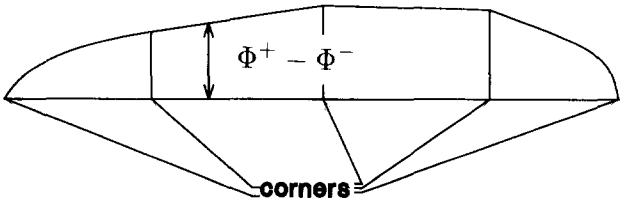

Fig. 3. Distribution of $(\Phi^+ - \Phi^-)$ along an open-ended boundary, as a function of distance along the boundary.

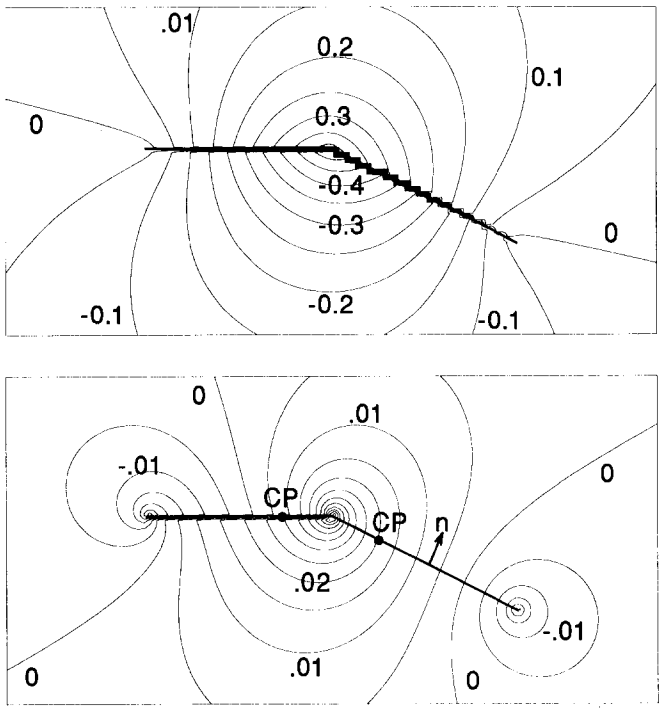

Fig. 4. Top: unit function potential Φ, contour interval 0.05. Bottom: component of aquifer discharge normal to the right-hand segment Q_n, contour interval 0.005 (CP denotes control point locations).

Boundary Conditions for an Impermeable Boundary

As discussed above, the unknowns that need to be determined are the potential differences $(\Phi^+ - \Phi^-)$ at each corner of the boundary, which in turn determine the constants a_0 and a_1 in (11) and (13) for each segment of the boundary. The desired boundary condition is zero aquifer discharge normal to the boundary, $Q_n = (Q_x, Q_y) \cdot n = 0$, where Q_n is the component of the aquifer discharge vector (Q_x, Q_y) normal to the boundary, and n is a unit vector normal to the boundary. For each unknown $(\Phi^+ - \Phi^-)$ at a corner, the equation generated involves the sum of normal flux at two control points straddling the corner.

$$Q_n(z_i) + Q_n(z_j) = 0 \tag{15}$$

where z_i and z_j are the complex coordinates of the two control points. The condition (15) causes close approximation of $Q_n = 0$ along the entire boundary, provided the boundary is broken into small enough segments.

Boundary Conditions for a Resistant Boundary

The condition applied to the resistant boundary control points is

$$Q_n(z_i) + Q_n(z_j) = Q_n^*(z_i) + Q_n^*(z_j) \tag{16}$$

where $Q_n(z_i)$ and $Q_n(z_j)$ are the components of modeled aquifer discharge normal to the boundary at the control points z_i and z_j. The terms $Q_n^*(z_i)$ and $Q_n^*(z_j)$ are the leakage rates through the boundary per unit length of boundary at the control points. Q_n^* is calculated as the gradient of a potential defined within the resistant barrier, Φ*, as though the barrier has finite width b* and hydraulic conductivity k*.

$$Q_n^* = -\frac{\partial \Phi^*}{\partial n} = \frac{\Phi^{*+} - \Phi^{*-}}{b^*} \tag{17}$$

where the + and − superscripts refer to opposite sides of the boundary. If the aquifer is unconfined,

$$\Phi^* = \tfrac{1}{2}k^*(\phi - b_1)^2 \quad \phi \le b_3 \tag{18}$$

and if it is confined

$$\Phi^* = k^*[(b_3 - b_1)(\phi - b_1) - \tfrac{1}{2}(b_3 - b_1)^2] \quad \phi \ge b_3 \tag{19}$$

where b_1 and b_3 are as defined in Figure 1. Equations (17) through (19) result in equation (36.1) of Strack (1989) when heads are unconfined on both sides of the boundary in a single-layer aquifer and equation (36.3) of Strack (1989) when heads are confined on both sides. The formulation presented here is more flexible than the formulation of Strack (1989), since it allows for nonlinear conditions with layered aquifers and changes from confined to unconfined flow across the boundary.

Combining equations (16) and (17) gives

$$Q_n(z_i) + Q_n(z_j) = \frac{1}{b^*}$$
$$[\Phi^{*+}(z_i) - \Phi^{*-}(z_i) + \Phi^{*+}(z_j) - \Phi^{*-}(z_j)] \tag{20}$$

The boundary condition equation (20) is put in terms of the aquifer potential by assuming a linear relationship

$$\frac{1}{b^*}[\Phi^{*+}(z_i) - \Phi^{*-}(z_i) + \Phi^{*+}(z_j) - \Phi^{*-}(z_j)] =$$
$$M[\Phi^+(z_i) - \Phi^-(z_i) + \Phi^+(z_j) - \Phi^-(z_j)] + N \tag{21}$$

where M and N are constants. Combining (20) and (21) gives

$$Q_n(z_i) + Q_n(z_j) =$$
$$M[\Phi^+(z_i) - \Phi^-(z_i) + \Phi^+(z_j) - \Phi^-(z_j)] + N \tag{22}$$

The constants M and N are determined by the head at the control points and relations (4), (18), and (19). The ratio b*/k* can always be factored out of the left side of (21), and is embedded in the constants M and N. The boundary is modeled as having no actual width, so the factor b*/k* is specified as the resistance of the boundary.

If the aquifer is confined on both sides of the boundary, or if the aquifer is unconfined in the lower layer on both sides of the boundary ($\phi \le b_2$ in Figure 1), the relation (21) is truly linear, and no iteration is required to solve the system of equations. In other cases, relation (21) is only a linear approximation of a nonlinear relationship, and iteration is required. With each iteration, estimates of the constants M and N are updated based on new estimates of heads on opposite sides of the boundary at the control points. Iteration proceeds until some closure criterion is met [e.g. the left and right sides of (16) differ by no more than 1%].

This method will cause close approximation of $Q_n = Q_n^*$ along the entire boundary, provided the boundary is broken into a sufficiently large number of segments (experience indicates that 10 to 30 segments per barrier is enough in most cases). Inherent in this two-dimensional formulation is the assumption that the resistance to vertical flow inside the barrier can be neglected; this assumption is generally valid if the barrier is thin and the saturated thickness does not change dramatically across the barrier.

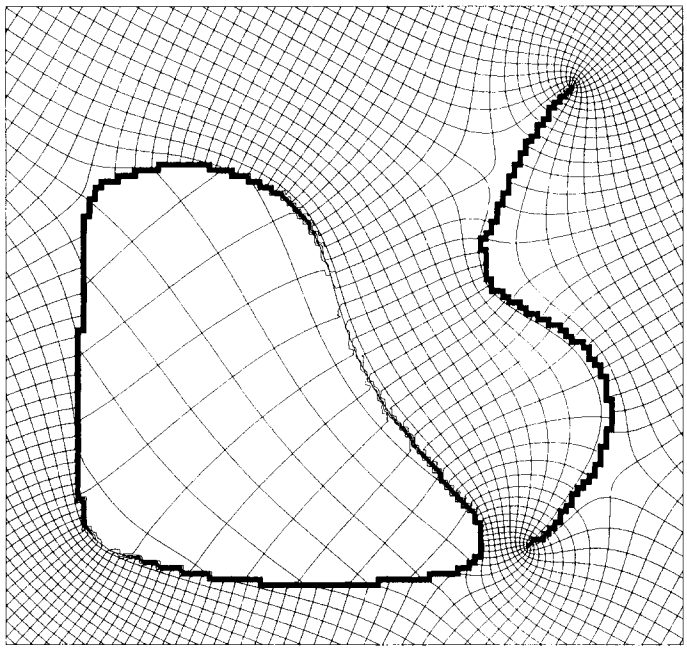

Fig. 5. Contours of Φ and Ψ. Contour interval 1.0 m^3/day.

Implementation

This method has been implemented by the author in the computer program TWODAN. TWODAN can superposition large numbers of analytic functions to represent variable infiltration/leakage, uniform crossflow, point sources or sinks (wells), line sources or sinks (streams), aquifer heterogeneities, impermeable barriers, and resistant barriers. The program uses the composite analytic solution to directly generate contour plots and pathlines.

A model constructed to check implementation contains a closed resistant boundary formed of 42 line segments and an open impermeable boundary formed of 23 line segments. The aquifer has two layers; the lower layer is 4 m thick with hydraulic conductivity of 3 m/d and the upper layer is 1 m thick with hydraulic conductivity of 12 m/d. The model consists of the functions representing the two boundaries plus the potential for a uniform flow with $Q_{x0} = 0.153$ m^2/d and $Q_{y0} = -0.129$ m^2/d.

$$\Phi_{uni} = -Q_{x0}x - Q_{y0}y \qquad (23)$$

The closed boundary is resistant with resistance $b^*/k^* = 100$ days. The open boundary is an impermeable one.

An analytic flow-net of the solution is shown in Figure 5. The flow-net was produced by contouring the composite Φ and Ψ functions, using a contour interval of 1.0 m^3/day for both functions. The contour interval represents the discharge between adjacent stream function contours (streamlines). To create this plot, the analytic solution was evaluated at about 13,500 regularly spaced points within the plot area, and these data were contoured with a linear interpolation algorithm. Where head drops across the boundaries, the potential is discontinuous. The flow-net illustrates that the solution is indeed analytic, and that there is perfect continuity of flow through and around the boundaries (the stream function is continuous). Along the impermeable boundary, the streamlines indicate that the solution closely approximates the no-flow boundary condition. The heads along both boundaries vary from fully confined conditions at the upstream end (top of Figure 5) to unconfined in the lower layer at the downstream end (bottom), to test the full range of possible head-potential relationships.

A utility of TWODAN checks how well the solution meets the boundary conditions at each corner, namely equation (15) for the impermeable boundary and equation (16) for the resistant boundary. For all corners of the impermeable boundary, $|Q_n(z_i) + Q_n(z_j)| < 4.1 \times 10^{-7}$ m^2/day. For all corners of the resistant boundary, $Q_n(z_i) + Q_n(z_j)$ differed from $Q_n^*(z_i) + Q_n^*(z_j)$ by less than 0.07%.

To demonstrate that the solution is not highly dependent on the discretization of line segments representing the boundaries, a second model was developed which is identical to the one that produced Figure 5, except that the boundaries are represented by about half as many segments (22 for the resistant boundary and 11 for the impermeable one). The analytic flow-net for this model is shown in Figure 6. Although there are slight differences in the patterns close to the boundaries, both portray essentially the same flow-field.

Application to "Funnel and Gate" Barrier Systems

Application of this method is demonstrated in models of what have been called "funnel and gate" remediation systems. In these systems, barriers funnel contaminated ground water through a narrow gap or "gate," where the water can be treated in situ in a limited area (Pankow et al., 1993). The barriers would typically be slurry walls or sheet-pile walls that key into an aquitard at the base of the aquifer.

Five barrier configurations were modeled, with results shown as analytic flow-nets in Figure 7. Since the flow-nets are symmetric about the bisecting line between the two barriers, only the left half is shown. Each model contains analytic functions representing the barriers and a function representing uniform flow in the negative y direction. Each barrier is represented as an impermeable boundary with 9 to 17 segments, an upstream opening width L, and a downstream opening width l. In all cases, the aquifer was confined with the same fixed transmissivity T.

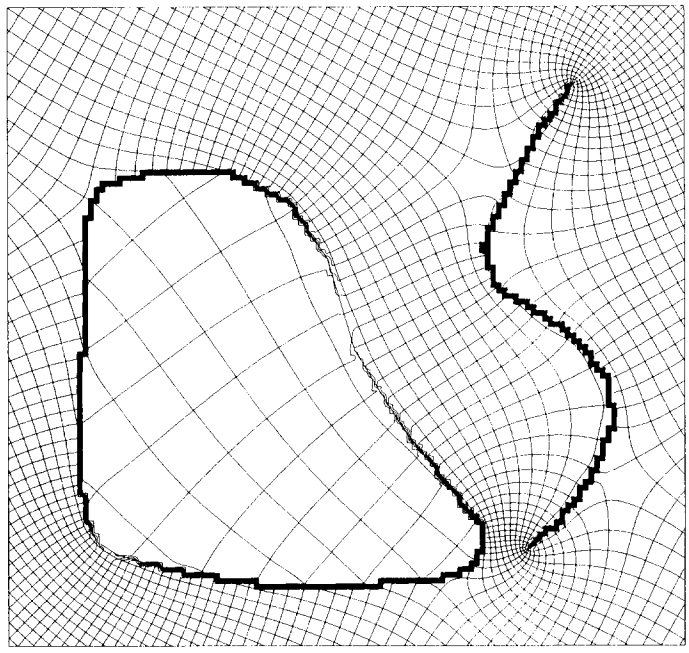

Fig. 6. Same as Figure 5, but with fewer segments representing the boundaries.

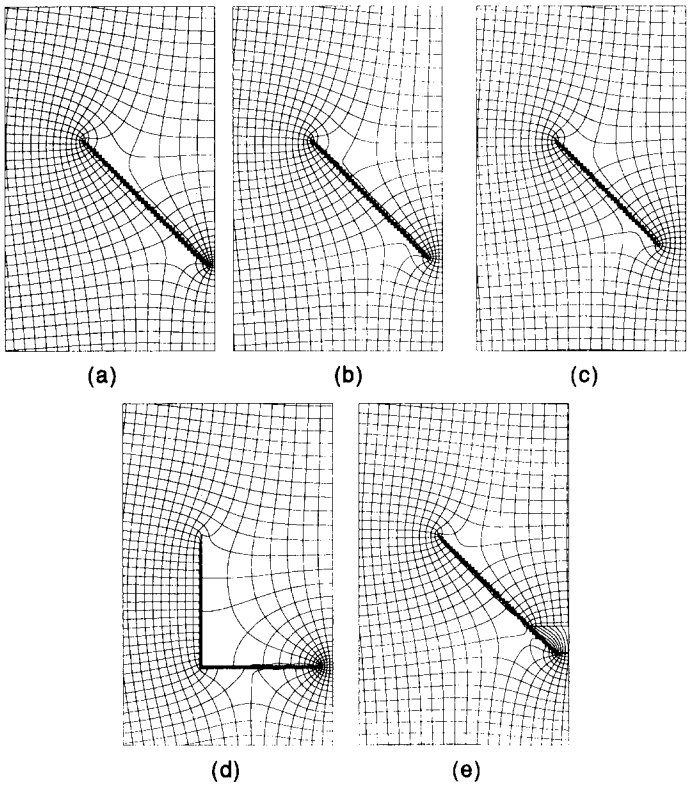

Fig. 7. Analytic flow-nets for five impermeable barrier configurations.

Configurations (a), (b), and (c) contain two straight barriers at 45 degrees to the incoming flow, with gap widths of $l = 0.05L$, $0.1L$, and $0.2L$, respectively. Configuration (d) has a gap width of $l = 0.1L$, but a rectangular barrier arrangement. Configuration (e) is like (a), except there is a trapezoidal region in the gate area where the transmissivity is 100 times higher than the surrounding aquifer transmissivity. Such high transmissivity zones may be constructed to provide a zone where oxygen or other chemical agents could be introduced to enhance remediation. The technique for modeling heterogeneity boundaries is not discussed here, but is covered by Strack and Haitjema (1981b), Fitts (1985), and Strack (1989).

The flow-nets of Figure 7 provide some insights for design of "funnel and gate" barrier systems. The results for all five cases indicate that the zone of water captured and funneled through the gate narrows substantially upstream of the barriers, because some flow is forced out and around the barriers. At a distance $L/2$ upstream of the upstream opening of the barriers, the width of flow captured ranged from about $0.4L$ in case (a) to about $0.55L$ in case (c). These results indicate that the upstream opening width L should be designed substantially wider than the plume that the barriers are intended to capture. Although the gap in case (c) is four times larger than the gap in case (a), the flow through the gap in case (c) is only about 40% larger than in case (a); this is the result of higher velocities in the gap as the gap width l decreases. Configurations (b) and (d) both have gap widths of $l = 0.1L$, but the flow through the gap in (d) is about 30% larger than the flow through the gap in (b). The high transmissivity zone of model (e) reduces resistance in the gap area, and allows 25% more flow through the gap than the comparable homogeneous model (b).

Concluding Remarks

The method presented here allows efficient and accurate modeling of barriers in two-dimensional steady flow. To set up a model with a barrier, the user only has to specify the verticies of the boundary line segments and possibly a resistance. The models presented in Figures 5, 6, and 7 were created in just a few minutes. To be more specific, the following times apply for these models, using standard personal computer equipment (60 MHZ pentium PC): defining the boundaries took less than 5 minutes (it was done graphically), solving the system of equations took less than 15 seconds, and generating the contour plots on screen required less than one minute. To develop similar models with numerical methods, the user must define fine discretization near the boundary and specify the properties of all elements of the boundary and vicinity; this process can be very time-consuming. The efficiency advantage of this method over numerical methods becomes especially important if the model is used in design mode to test various barrier configurations.

This approach does have some limitations, one of which is that it is steady, not transient. Development of fully analytic methods for barriers in transient flow is unlikely, due to the difficulty of finding and implementing analytic solutions which can meet complex boundary conditions in space and time. Another limitation is that the present implementation in TWODAN does not allow barrier boundaries to cross heterogeneity boundaries. It is theoretically possible to allow such crossings, and such capability may some day be implemented.

References

Fitts, C. R. 1985. Modeling aquifer inhomogeneities with analytic elements. M.S. thesis, Univ. of Minnesota, Minneapolis.

He, H. Y. 1987. Groundwater modeling of leaky wall. M.S. thesis, Univ. of Minnesota.

Hsieh, P. A. and J. R. Freckleton. 1993. Documentation of a computer program to simulate horizontal-flow barriers using the U.S. Geological Survey modular three-dimensional finite difference ground-water flow model. U.S. Geological Survey Open-File Report 92-477.

McDonald, M. G. and A. W. Harbaugh. 1988. A modular three-dimensional finite difference ground-water flow model. Techniques of Water Resources Investigations of the U.S. Geological Survey. book 6, chapter A1.

Pankow, J. F., R. L. Johnson, and J. A. Cherry. 1993. Air sparging in gate wells in cutoff walls and trenches for control of plumes of volatile organic compounds (VOCs). Ground Water. v. 31, no. 4, pp. 654-663.

Strack, O.D.L. 1989. Groundwater Mechanics. Prentice-Hall, Englewood Cliffs, NJ.

Strack, O.D.L. 1986. Curvilinear analytic elements. Report on Research done for the U.S. Bureau of Mines, Minneapolis.

Strack, O.D.L. and H. M. Haitjema. 1981a. Modeling double aquifer flow using a comprehensive potential and distributed singularities; 1. Solution for homogeneous permeability. Water Resources Research. v. 17, no. 5, pp. 1535-1549.

Strack, O.D.L. and H. M. Haitjema. 1981b. Modeling double aquifer flow using a comprehensive potential and distributed singularities; 2. Solution for inhomogeneous permeabilities. Water Resources Research. v. 17, no. 5, pp. 1551-1560.